On the sensitivity of ultrasonic welding of epoxy- to polyetheretherketone (PEEK)-based composites to the heating time during the welding process

Tsiangou, Eirini; Kupski, Julian; Teixeira de Freitas, Sofia; Benedictus, Rinze; Villegas, Irene Fernandez

DOI
10.1016/j.compositesa.2021.106334

Publication date
2021

Document Version
Final published version

Published in
Composites Part A: Applied Science and Manufacturing

Composites: Part A 144 (2021) 106334

Contents lists available at ScienceDirect

Composites Part A

journal homepage: www.elsevier.com/locate/compositesa

On the sensitivity of ultrasonic welding of epoxy- to polyetheretherketone (PEEK)-based composites to the heating time during the welding process

Eirini Tsiangou *, Julian Kupski, Sofia Teixeira de Freitas, Rinze Benedictus, Irene Fernandez Villegas

Aerospace Structures and Materials Department, Faculty of Aerospace Engineering, Delft University of Technology, Kluyverweg 1, 2629HS Delft, the Netherlands

ARTICLE INFO

Keywords:
A. Polymer-matrix composites (PMCs)
A. Thermoplastic resin
A. Thermosetting resin
E. Joints/joining

ABSTRACT

This study aims at assessing the sensitivity of the ultrasonic welding process for joining epoxy- to thermoplastic-based composites sensitivity to the heating time. For that, carbon fibre (CF)/epoxy adherends with a co-cured PEI coupling layer were ultrasonically welded to CF/polyetheretherketone (PEEK) adherends at different heating times. Process-induced changes in the meso and microstructure of these welds were identified and correlated to the weld strength. Subsequently, a processing interval, i.e., a range of heating times resulting in less than 10% decrease of weld strength, was defined. As, expected, the dissimilar composite welded joints were more sensitive to the heating time than the CF/PEEK to CF/PEEK welded joints. However, this effect was less pronounced than expected, since a relatively wide processing interval could be obtained provided that the coupling layer had a sufficient thickness.

1. Introduction

Owing to the fact that welding of composite materials is a very attractive alternative to mechanical fastening (drilling holes) and adhesive bonding (excessive surface pre-treatment, long curing cycles) [1], research on welding of composites is not only limited to thermoplastic but also thermoset composites. One of the most efficient ways to make thermoset composites (TSC) weldable is by attaching a compatible thermoplastic film, hereafter referred to as coupling layer, on top of the un-cured TSC laminate and curing them together [2]. The TSC can be afterwards fusion bonded or welded through this thermoplastic film. Fusion bonding techniques to join TSC parts have been successfully applied by different research groups and include co-consolidation in an oven [3–5], resistance welding [6–8], induction welding [9,10], vibration welding [11] and ultrasonic welding [2,10,12–14]. Out of these fusion bonding techniques, ultrasonic welding might be the most promising one, since the risk of thermal degradation of the thermoset resin can be rather limited by its exceptionally short heating times. The risk of overheating of the thermoset resin can be significant, especially if thermoplastic resins with high melting temperatures are used (e.g. PEEK). Based on previous findings, we believe that very fast (less than 500 ms) and localized heating can decrease such risk, even if high welding temperatures are reached [12]. Moreover, ultrasonic welding is an excellent technique for joining composites, as it can provide strong joints in a rather fast and cost-effective way [15].

Villegas and Rubio in [12] investigated the effect of the heating time on the quality of (CF)/epoxy to CF/polyetheretherketone (PEEK) joints ultrasonically welded either directly or through a PEEK coupling layer by changing the welding force and amplitude of the vibrations. They showed that a combination of high force and amplitude results in very short heating times which in turn helps to prevent thermal degradation of the epoxy resin. Villegas and van Moorleghem investigated in [2] ultrasonic welding of CF/epoxy to CF/PEEK composites through a polyetherimide (PEI) coupling layer. Their study focussed on the analysis of the morphology of the interphase formed between the PEI and epoxy resins, on the effect of the ultrasonic welding process on this interphase and they also showed promising results from single-lap shear testing of the welded joints. In a side study, they also demonstrated that lack of combatibility between a PEEK coupling layer and the epoxy resin resulted in a clear boundary after the co-curing process and poor durability of the connection. Ultrasonic welding was used to weld two CF/epoxy adherends through poly-vynil-butyral (PVB) films in a study by Lionetto et al. [10], in which comparison with specimens welded by means of induction welding showed that ultrasonic welding can produce welds with higher strength. In our previous work, we investigated the possibility of welding CF/epoxy to CF/PEI specimens solely through the

* Corresponding author.
E-mail address: E.Tsiangou@tudelft.nl (E. Tsiangou).

https://doi.org/10.1016/j.compositesa.2021.106334
Received 14 December 2020; Received in revised form 9 February 2021; Accepted 13 February 2021
Available online 19 February 2021

coupling layer, and concluded that an energy director (ED) is required at the interface to help promote heat locally, without risking excessive bulk heating [13]. In that particular study a 250 μm-thick flat PEI ED was used. The lap shear strength (LSS) of CF/epoxy and CF/PEI specimens welded through a PEI ED and a 60 μm-thick PEI coupling layer was similar to that of reference co-cured CF/epoxy to CF/PEI specimens. Finally, our results in [14] showed that for welding of CF/epoxy to CF/PEEK adherends a 250 μm-thick coupling layer results in better mechanical performance as compared to a 60 μm-thick one. In particular, specimens provided with a 250 μm-thick coupling layer resulted in a LSS comparable to that of reference CF/PEEK to CF/PEEK welded specimens. Compared to the study mentioned before in which a 60 μm-thick coupling layer together with a 250 μm-thick PEI ED were found sufficient for the production of high-strength welds [13], the PEEK matrix has a higher melting temperature than the softening temperature of PEI, which increases the risk of thermal degradation of the epoxy resin. Nevertheless, the results obtained in all the mentioned studies show how promising ultrasonic welding is for dissimilar composite joints.

To further assess the applicability of ultrasonic welding to dissimilar composites joints, it is however important to ascertain how sensitive the weld quality is to variations in the process parameters (welding force, vibrations amplitude and/or heating time), especially taking into account how critical it seems to be to keeping the heating time short [12]. As a first step to fill this knowledge gap, this study focuses on investigating the effects of the heating time on the meso and microstructure of dissimilar composite (CF/epoxy to CF/PEEK) welded joints and their relation to the weld strength. Meso and microstructures were assessed via cross-sectional microscopy and the weld strength was assessed through single-lap shear tests. Relations between structure and strength were established with the help of fractography and by modelling the stress distribution along the welded overlap in the specific joints under study. Furthermore, a processing interval was defined with respect to the shortest and longest heating times that resulted in a minimum target weld strength for different coupling layer thicknesses. The processing intervals of the considered dissimilar composite welded joints were then compared to that of a reference CF/PEEK to CF/PEEK welded joints.

2. Experimental procedure

2.1. Materials and manufacturing

In this study, Cetex® CF/PEEK (carbon fibre/polyetheretherketone) prepreg with a 5-harness satin fabric reinforcement, manufactured by Toray Advanced Composites (the Netherlands) was used as the TPC adherend. CF/PEEK prepreg plies arranged in a $[0/90]_{3s}$ stacking sequence were consolidated in a hot-platen press at 385 °C and 1 MPa for 30 min. The thickness of the consolidated laminates was approximately 2 mm.

A T800S/3911 unidirectional CF/epoxy particle-toughened prepreg (provided by TORAY (Japan)) was used to manufacture the TSC adherend. PEI films with thicknesses of 60 μm (SABIC, the Netherlands), 175 μm and 250 μm (LITE, Germany) were used as the different coupling layers in this study and were co-cured to the surfaces of the CF/epoxy laminates. The maximum thickness of 250 μm was chosen based on the results obtained in [14]. Note that the 175 and 250 μm-thick films were placed on both sides of the laminates, since otherwise the cured laminates were warped, possibly because of different thermal expansion coefficient of the CF/epoxy and PEI materials. The PEI coupling layers were degreased with isopropanol prior to their application on the prepreg stack. The CF/epoxy laminates ($[0/90]_{2s}$ stacking sequence) provided with the coupling layer(s) were cured in an autoclave at 180 °C and 7 bars for 120 min, according to the specifications of the manufacturer. To ensure smooth surfaces on both sides of the laminate an aluminium caul plate was used on the side of the vacuum bag. The final thickness of the CF/epoxy/PEI laminates was approximately 2.15 mm, 2.45 mm and 2.6 mm for the 60, 175 and 250 μm-thick coupling layers, respectively. In our previous study [13] we found that an approximately 25 μm-thick gradient epoxy/PEI interphase was formed between these epoxy and PEI materials during the curing process. The gradient interphase consisted of epoxy spheres dispersed in the PEI resin. The diameter of these spheres was smaller closer to the PEI film than in the region with high epoxy resin content. More information on this gradient interphase can be found in [13]. The amorphous PEI resin has low solvent resistance and might pose a threat to the durability of the welded joints in specific applications. Further work should be performed to understand potential limitations imposed by the use of an amorphous polymer as a coupling layer, however this was out of the scope of this study.

A water-cooled circular diamond saw was used to cut the CF/PEEK and CF/epoxy/PEI laminates into 25.4 mm × 106 mm adherends with their longitudinal direction parallel to the main apparent orientation and to the 0° orientation of the fibres, respectively.

2.2. Welding process

The adherends were welded with a HiQ DIALOG SpeedControl ultrasonic welder (Herrmann Ultraschal, Germany). In order to keep the adherends in place during welding, the same custom-made jig as in [14] was used. The adherends were welded in a single-lap configuration with a 12.7 mm long and 25.4 mm wide overlap using a 250 μm-thick flat PEEK film (provided by Victrex, the Netherlands) as energy director (ED). The PEEK ED was fixed on top of the CF/epoxy/PEI adherend using adhesive tape. Based on our previous study [13], a loose ED was added in addition to the coupling layer in order to avoid overheating of the coupling layer and/or adherends. A rectangular sonotrode with dimensions 30 × 16 mm was utilized. The welding force and peak-to-peak amplitude of vibrations used in this study were 1200 N and 86 μm, respectively. The solidification force and time were kept constant at 1200 N and 4 s, respectively. Displacement-controlled welding was used, i.e. the heating time was indirectly controlled by the downward displacement of the sonotrode [16]. The actual heating time was provided as output by the welder at the end of each welding process. The different welding configurations considered in this study together with the different displacement values at which the vibration phase was stopped in each configuration are listed in Table 1. The effect of the heating time on the mesostructure and microstructure and their relation to the weld strength were assessed for the epoxy-PEEK 250 specimens and compared to the reference PEEK-PEEK configuration. Additionally, processing intervals (see Section 2.3) were defined for all configurations in Table 1.

2.3. Testing and analysis

Optical microscopy (Zeiss Axiovert 40 optical microscope) together with scanning electron microscopy (SEM, JEOL JSM-7500F scanning electron microscope) were used for cross-sectional analysis of as-welded specimens. Cross-sectional analysis was performed in order to observe the meso- and microstructure of specimens welded at different

Table 1
Welding configurations considered in this study and respective displacement values at which the vibration phase was stopped. At least 5 samples were welded per configuration and displacement value.

Configuration	Coupling layer thickness (μm)	Displacement values (mm)
Epoxy-PEEK 250	250	0.2, 0.22, 0.24, 0.26, 0.28, 0.3, 0.32, 0.34, 0.36, 0.38
Epoxy- PEEK 175	175	0.16, 0.18, 0.2, 0.22, 0.24, 0.26, 0.28, 0.3, 0.32
Epoxy- PEEK 60	60	0.11, 0.13, 0.15, 0.17
PEEK-PEEK	–	0.1, 0.12, 0.14, 0.16, 0.18, 0.2, 0.22, 0.24

displacement values. The specimens were cut at the middle of the overlap and perpendicular to the 0° fibres on the outer surfaces of the CF/epoxy adherend.

Single lap shear tests were performed according to the ASTM D 1002 standard in a Zwick 250 kN universal testing machine. The lap shear strength (LSS) of the joints was calculated as the maximum load divided by the overlap area. Five specimens were welded in each welding configuration and displacement value (see Table 1) and the resulting LSS values were used to determine the average LSS and standard deviation for each case. Naked eye observation and SEM were used for the fractographic analysis of the welded joints after mechanical testing. Naked eye observation was found adequate to identify the most relevant features on the fracture surfaces. SEM was used to provide details on a micro level to confirm the naked-eye observations.

A processing interval was defined for displacement values that resulted in welds with an average LSS higher than 90% of the maximum average LSS achieved within each configuration. Note that a similar practice was followed by Hou et al. in [17] to determine a processing window for resistance welding of CF/PEI samples. In that study, the LSS of the considered welded configurations was however compared to that of compression moulded benchmark samples.

3. Finite element model

Considering the known effect of the bond line thickness on the LSS of adhesively bonded joints [18], it was expected that the varying weld line thickness with varying sonotrode displacement (or heating time) would similarly play a role in the LSS of the welded joints. In order to assess the effect of the weld line thickness on the peel and shear stresses in the epoxy-PEEK 250 welds during testing, a FE-model was built. Fig. 1 illustrates the 3D FE-model built in Abaqus, including dimensions and boundary conditions. The model was representative of the lap shear test, with one end having nodes fixed in 3 degrees of freedom, while on the other end, solely longitudinal displacement was allowed. Fig. 2 shows the mesh at the overlap which was thinner towards the weld line and towards the edges of the overlap. A spew fillet was also included in the model as a representation of the resin squeeze-out that was observed in all epoxy-PEEK 250 specimens. The spew fillet was designed with a 45° slope and a height reaching half the adherend's thickness as a rough approximation of what was observed on the welded specimens. It should be noted that, since the fillet in the welded joints was formed by resin flowing out of the weld line without any specific restriction, its shape was quite irregular, hence the triangular shape of the fillet in the model was an over simplification. However, since our interest was on comparing the peak stress values corresponding to different weld line thicknesses rather than on the absolute values themselves, we considered this oversimplification to not have a significant effect on our analysis. The weld line was modelled with three thicknesses, 0.2, 0.1 and 0.05 mm. These thicknesses were based on the cross-sectional micrographs of epoxy-PEEK 250 specimens that resulted in significantly different LSS, as it will be shown in Sections 4.1 and 4.3. The weld line was modelled with a consistent element height of 0.05 mm for all topology configurations, which results in 4 elements through the thickness for 0.2 mm, 2 elements for 0.1 mm, and 1 element for 0.05 mm-thick weld lines. The element thickness inside the adherends was decreased towards the weld line. The outside half of the adherends was modelled with one element per single layer through the thickness, resulting in 0.3 mm for a single layer of CF/PEEK woven fabric and in 0.25 mm for a single UD layer of CF/epoxy prepreg. The inside half of the adherends, alongside the fillet, was modelled with the element height used in the weld line, 0.05 mm.

In order to guarantee that the results were mesh-independent, a mesh convergence study was performed by comparison of different element types C3D8R, C3D8 and C3D20R (all elements have three active degrees of freedom, i.e., translations in the x, y and z directions), with constant number of elements. A sufficient convergence could be established with element type C3D8R. The length of one element in the area around the spew fillet was set to 0.05 mm and the width to 0.1 mm, gradually increasing towards the top and bottom edges of the overlap. This mesh design resulted in a total mesh size of 1,082,633 elements for the 0.2 mm-thick weld line, 1,055,956 elements for the 0.1 mm-thick weld line and 1,040,300 elements for the 0.05 mm-thick weld line.

The adherends were modelled as linear elastic, based on the properties listed in Table 2. The PEI coupling layer and the ED were modelled as linear-elastic/plastic, using the values in Table 3. Note that even though the ED used in the experiments was made out of PEEK, it was decided to model it as a PEI ED for simplicity. This decision was based on the fact that both ED materials resulted in similar LSS and failure locus in our previous research [14]. The load was applied in a single step taking into account non-linear geometry effects.

4. Results

4.1. Mesostructure and microstructure

Fig. 3 shows cross-sectional micrographs from epoxy-PEEK 250 specimens welded at 0.20 mm (corresponding to 425 ± 37 ms heating time), 0.30 mm (461 ± 38 ms) and 0.38 mm (643 ± 36 ms). The relevance of these displacement values relative to weld strength will be shown in Section 4.3. Two main observations regarding the mesostructure of the welded joints can be made from these figures. Firstly, the weld line thickness, defined as the amount of neat resin between the topmost CF bundles in the two adherends, decreased, as expected, with increasing displacement or heating time. Weld line thicknesses of approximately 200 μm, 100 μm, and 50 μm were measured at 0.20 mm, 0.30 mm and 0.38 mm displacement, respectively.

Secondly, the contribution of the PEI coupling layer and of the PEEK energy director to the weld line, which could be discerned given the different shades of grey featured by the PEI and the PEEK resins under the optical microscope, changed with the displacement of the sonotrode.

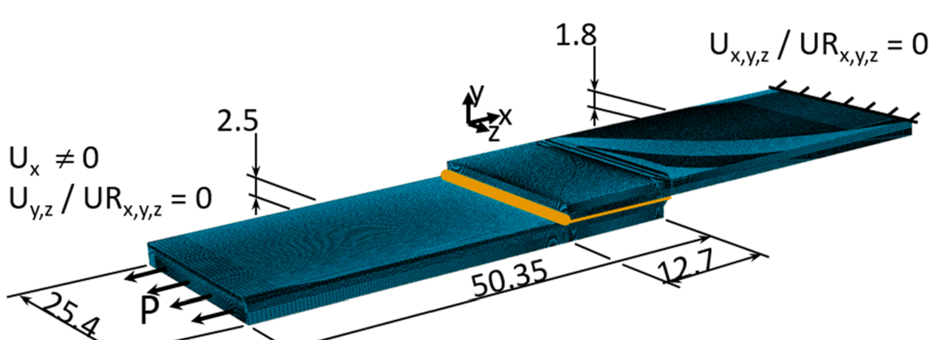

Fig. 1. 3D FE-model of the epoxy-PEEK 250 sample in a single-lap configuration, with boundary conditions. Dimensions are in [mm]. (For interpretation of the references to color in this figure legend, the reader is referred to the web version of this article.)

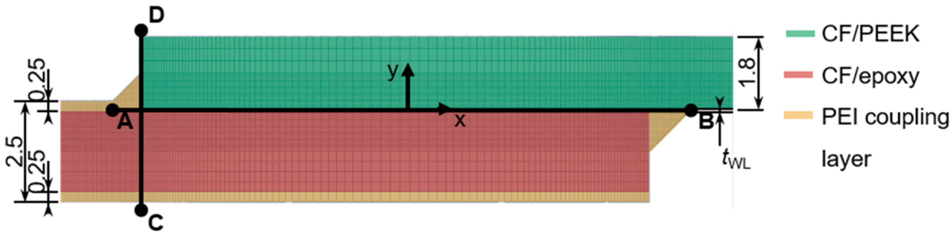

Fig. 2. 3D FE-model, central joint region for a single-lap design. The AB and CD paths correspond to the paths at which the peel and shear stresses were obtained. Dimensions are in [mm]. (For interpretation of the references to color in this figure legend, the reader is referred to the web version of this article.)

Table 2
Material properties of TENCATE CETEX TC1200 PEEK 5HS and TORAY T800S/3911 prepreg systems.

Property	Specification	CF/PEEK	CF/epoxy
Longitudinal tensile modulus (MPa)	E_{11}	56100[a]	172000[c]
Transverse tensile modulus (MPa)	E_{22}	55600[a]	8000[c]
Out-of-plane tensile modulus (MPa)	E_{33}	10000[b]	8000[c]
In-plane shear modulus (MPa)	$G_{12} = G_{13}$	4500[a]	5000[b]
Transverse shear modulus (MPa)	$G_{23} = E_{33}/(2(1 + \nu_{23}))$	3846	3077
In-plane Poisson ratio	$\nu_{12} = \nu_{13}$	0.27[b]	0.27[b]
Transverse Poisson ratio	ν_{23}	0.30[b]	0.30[b]

[a] TDS TENCATE CETEX TC1200 PEEK 5HS laminate.
[b] assumption, based on similar material Hexply 8552, Camanho et al. [19].
[c] provided by manufacturer TORAY (Japan).

Table 3
Material properties of ULTEM 1000 PEI resin.

Property	Specification	Value
Tensile modulus	E_{neat}	3280 MPa[a]
Tensile yield stress	σ	105 MPa[a]
Poisson ratio	ν_{neat}	0.36

[a] TDS ULTEM 1000.

In the sample welded at 0.20 mm displacement roughly two thirds of the total weld line (140 μm) consisted of PEI, i.e., coupling layer, while about one third (60 μm) consisted of PEEK, i.e., energy director and possibly matrix in the CF/PEEK adherend (Fig. 3a). Thus, about 45% of the PEI coupling layer and at least 75% of the PEEK ED were squeezed-out of the weld line. The exact amount of the PEEK squeeze-out cannot be determined since also PEEK matrix from the CF/PEEK adherend is present. However, in specimens welded at and above 0.30 mm (Fig. 3b and c) the energy director seemed to have been completely squeezed-out, resulting in a PEI-rich weld line. In some cases, such as clearly shown in Fig. 3b, the coupling layer was found to even flow in between the fibre bundles of the first layer of the CF/PEEK adherend.

With respect to the microstructure of the epoxy-PEEK 250 welds, increasing the displacement of the sonotrode above a certain threshold affected the condition of the gradient epoxy-PEI interphase originally formed during curing of the CF/epoxy adherends [13]. As seen in Fig. 4a, at 0.38 mm displacement the morphology of the interphase was affected by the welding process and featured bands of epoxy spheres interspersed with PEI-rich bands. This disruption of the interphase did however not happen at lower displacement values (0.30 mm and below), as seen in Fig. 4b.

Finally, Fig. 5 shows cross-sectional micrographs of PEEK-PEEK specimens welded at 0.12 mm (439 ± 31 ms), 0.18 mm (609 ± 37 ms) and 0.24 mm (734 ± 33 ms). The thickness of the weld line of PEEK-PEEK welded specimens decreased from approximately 90 μm for specimens welded at 0.12 mm to 70 μm at 0.18 mm, and finally to approximately 0 μm at 0.24 mm.

4.2. Weld line thickness and stress distribution

Fig. 6 shows the stress distributions obtained from the FE-model at a load of 3.3 kN. The value of 3.3 kN was defined in order to remain within the region before damage initiation occurred in the welded joints. This load corresponded to approximately 40% of the lowest failure load that was reached during mechanical testing of the epoxy-PEEK 250 welded specimens. Fig. 6a and b present the shear and peel stresses along the middle of the weld line for the weld line thicknesses of 50 μm, 100 μm and 200 μm measured on the cross-section micrographs in Section 4.1 (Fig. 3). As seen in Fig. 6a, the shear stresses were not affected by the thickness of the weld line for the thickness values considered. However, the peak peel stresses at the edges of the overlap increased with decreasing weld line thickness. Hence the 100 μm-thick weld line resulted in peak peel stresses that were 18% higher than the ones in the 200 μm-thick weld line. Moreover, in the 50 μm-thick weld line the peak peel stresses were around 93% higher than those in the 200 μm-thick weld line. This increasing trend is also seen in Fig. 6c, in which the peel stresses across the weld line are shown.

4.3. Processing interval

Fig. 7 illustrates the average LSS values obtained for the epoxy-PEEK 250 and reference PEEK-PEEK specimens welded at the displacement values defined in Table 1. Table 4 summarizes the results pertaining the definition of the processing intervals for these two configurations. The processing interval was defined to include the displacement values that resulted in an average LSS higher than the LSS threshold (defined as 90% of the maximum LSS in each configuration). In Table 4, the d_{opt} refers to the displacement value that resulted in the maximum average LSS. The limits d_{low} and d_{high} correspond to the lowest and highest displacement that resulted in an average LSS above the LSS threshold, respectively.

4.4. Fractography

Fracture surfaces of representative epoxy-PEEK 250 specimens can be seen in Fig. 8. For specimens welded below d_{low}, the fracture surfaces featured un-welded areas, mostly found towards the middle of the overlap, which decreased in size with increasing target displacement. Epoxy-PEEK 250 specimens welded around the d_{opt} featured almost fully welded overlaps and first-ply failure in the CF/PEEK adherend. In a microscopic level, the main failure feature was ruptured PEEK resin closely following the topology of the CF fibres in the fibre bundles, as seen in Fig. 9a. Some broken fibres could as well be observed. Epoxy-PEEK 250 specimens welded at displacement values equal or higher than d_{high} featured failure in both adherends, with failure in the CF/epoxy adherend increasingly present for increasing displacement values. As seen in Fig. 9b, the failure in the CF/epoxy adherend was characterized by ruptured resin as well as exposed and broken fibres.

Fig. 10 presents the fracture surfaces of reference PEEK-PEEK welded

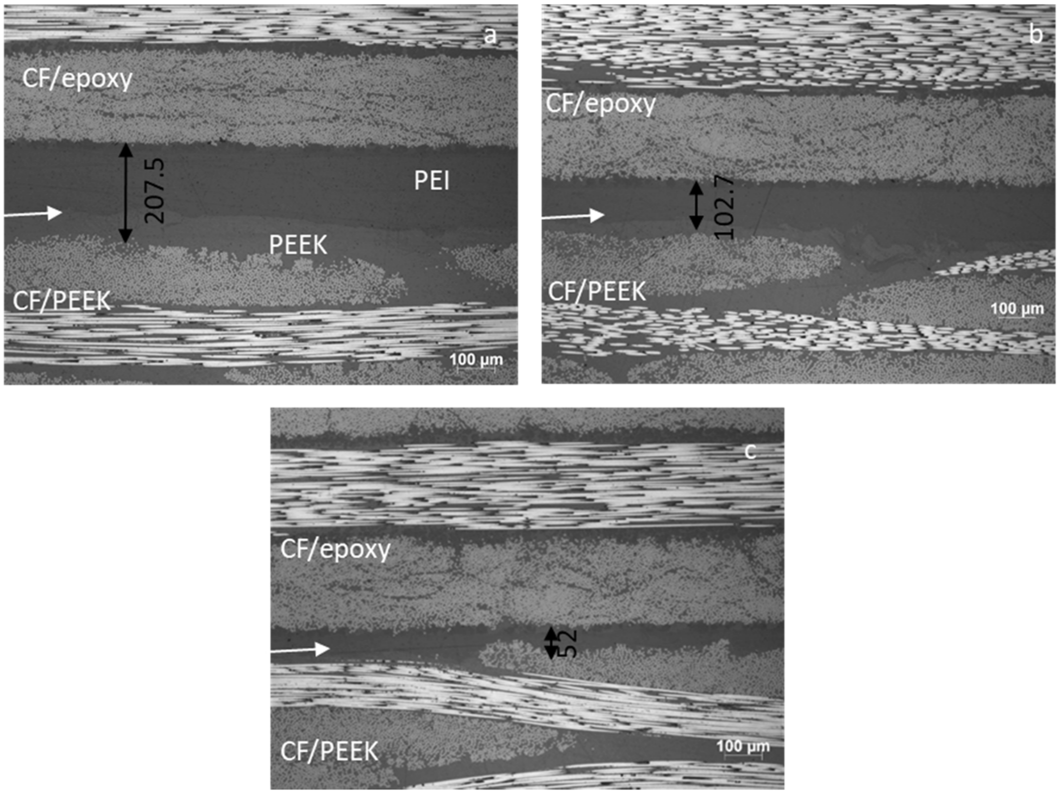

Fig. 3. Representative cross sections of epoxy-PEEK 250 samples welded at a displacement of a) 0.20 mm, b) 0.30 mm and c) 0.38 mm. The thickness of the weld line decreases with an increasing travel. White arrows indicate the weld line. The thickness measurements shown in the graphs are in μm.

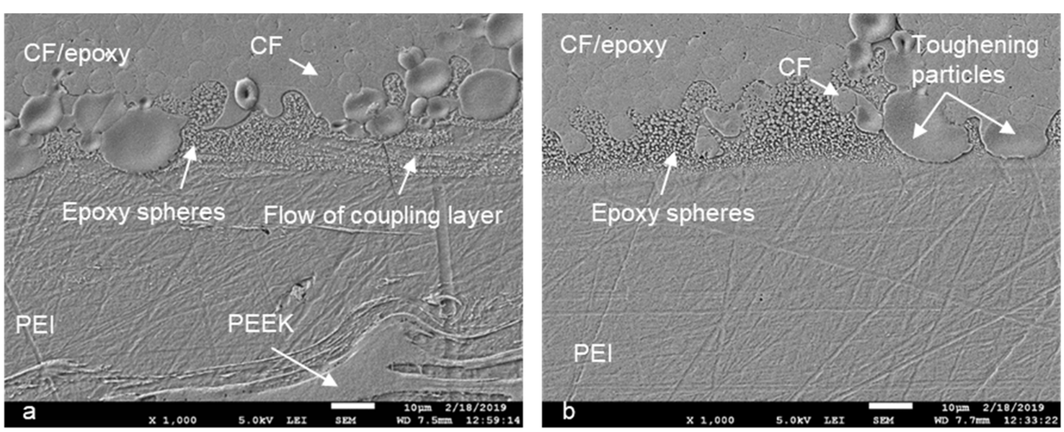

Fig. 4. Representative SEM cross-sectional micrographs of epoxy-PEEK 250 samples welded at a displacement of a) 0.38 mm and b) 0.30 mm. The epoxy-PEI interphase seems intact when samples are welded at d_{opt} whereas flow of the coupling layer close to the epoxy resin, leading to alteration of the original interphase morphology is observed when the samples are welded above d_{high}.

joints at different displacements. Below $d_{opt,}$ the reference PEEK-PEEK specimens featured un-welded areas that decreased in size with increasing target displacement. Reference PEEK-PEEK specimens welded at d_{low} still featured unwelded areas that covered approximately 20% of the total overlap. As seen in Fig. 11a, specimens welded at d_{opt} featured mostly fully welded overlaps and first-ply failure which was characterized by resin-rich failure within the CF bundles. Finally, in specimens welded at or right above d_{high}, distorted fibre bundles could be found at the edges of the overlap (Fig. 10). Additionally, instead of experiencing first-ply failure, the specimens failed between the first and second ply of one of the adherends. In a microscopic level, similar failure mechanisms as in reference PEEK-PEEK specimens were observed below and above d_{high}.

4.5. Coupling layer thickness

Decreasing the thickness of the coupling layer was expected to decrease the width of the processing interval, as a result of higher risk of thermal degradation of the CF/epoxy material. Fig. 12 presents the average LSS of the three considered epoxy-PEEK configurations, (i.e., epoxy-PEEK 250, epoxy-PEEK 175 and epoxy-PEEK 60 which were welded through a 250, 175 and 60 μm-thick coupling layer, respectively) plotted versus displacement. The results pertaining the definition of the processing interval for the epoxy-PEEK 175 configuration are summarized in Table 5. In the epoxy-PEEK 60 configuration, none of the considered displacement values resulted in an average LSS value above the established threshold. Note that the threshold considered for these

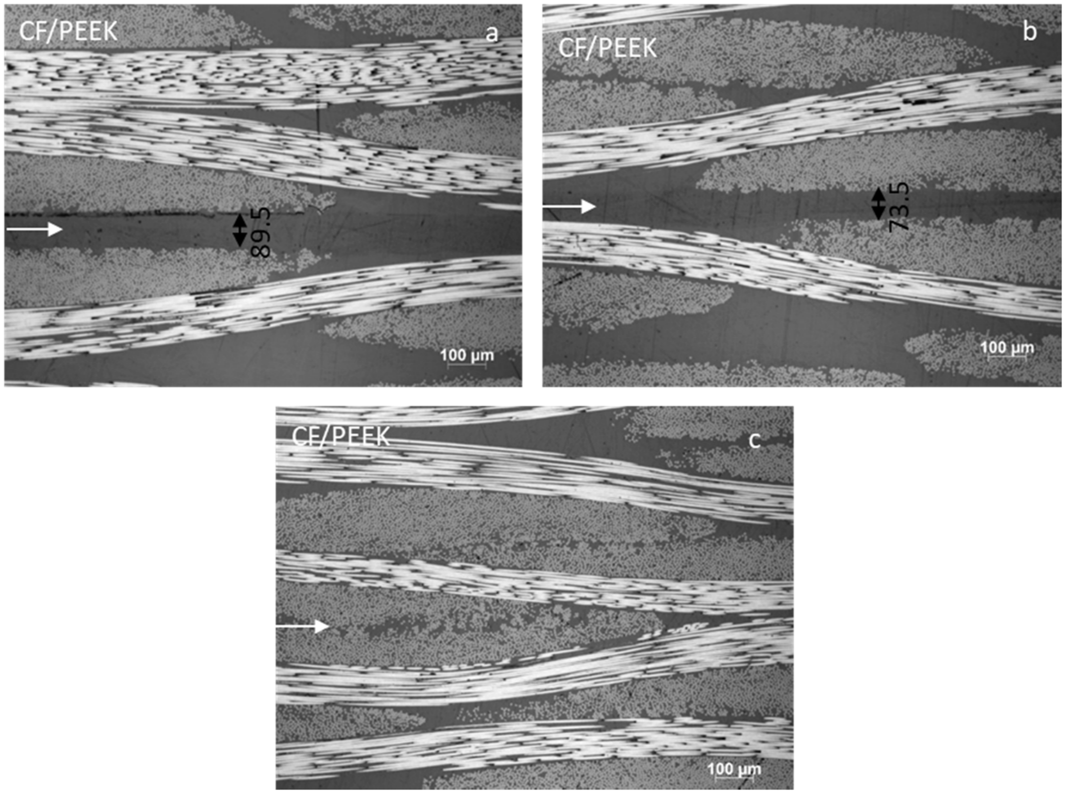

Fig. 5. Representative cross sections of reference PEEK-PEEK CF/PEEK samples welded at a displacement of a) 0.12 mm, b) 0.18 mm and c) 0.24 mm. The thickness of the weld line decreases with increasing displacement. White arrows indicate the weld line. The thickness measurements shown in the graphs are in µm.

three configurations was the same as defined for the epoxy-PEEK 250 configuration (see Table 4).

Fig. 13 presents fracture surfaces of epoxy-PEEK 175 specimens welded at different displacement values showing similar trends and features as the epoxy-PEEK 250 configuration. Closer inspection of the fracture surfaces of these specimens also showed similar failure mechanisms to those in the epoxy-PEEK 250 configuration. In the epoxy-PEEK 60 configuration, specimens that yielded the highest average LSS (at 0.13 mm) featured un-welded areas and failed partially in the CF/epoxy adherend. Welding at a higher displacement (0.17 mm) in order to achieve fully welded overlaps resulted in a lower LSS and predominant failure in the CF/epoxy adherend. These observations are consistent with the results presented in our previous study [14].

5. Discussion

The results presented in the previous section were interpreted in order to assess the effect of the heating time on the meso and microstructure of CF/epoxy to CF/PEEK specimens ultrasonically welded through a 250 µm-thick coupling layer (i.e., epoxy-PEEK 250 configuration). Relations between meso and microstructure and the weld strength were also analysed. Furthermore, a processing interval was defined with respect to the shortest and longest heating times that resulted in a minimum certain weld strength for different coupling layer thicknesses. The processing intervals of the considered dissimilar composite welded joints were then compared to that of a reference CF/PEEK to CF/PEEK welded configuration.

5.1. Relationship between meso and microstructure, and weld strength

Increasing the target displacement, thus the heating time, resulted in decreasing weld line thickness due to a higher amount of resin squeeze-out (Fig. 3). A direct correlation between the total amount of resin squeeze-out of at weld line and the target displacement could not be made due to resin being squeezed-out also from the top-most ply of the CF/PEEK adherend. Based on the FEM model, decreasing weld line thickness could have been expected to cause higher peel stresses in epoxy-PEEK 250 joints during testing (Fig. 6). Such results are in line with the study by Gleich et al. [18], in which a decrease in the failure load with increasing bondline thickness was shown for bondline thicknesses lower than 300 µm. However, decreasing the weld line thickness from 200 to 100 µm (between 0.20 and 0.30 mm displacement) caused the LSS to increase followed by a gradual drop for further decrease in the weld line thickness (Fig. 7). This initial increase in the LSS was attributed to the counteracting effect of increased welded area with decreased weld line thickness (Fig. 8). The subsequent decrease of the LSS was attributed not only to the potentially increased stresses during testing but also to a decrease in the coupling layer thickness (see Fig. 3). A decrease in the thickness of the coupling layer can be expected to increase the risk of thermal degradation of the CF/epoxy adherend, confirmed by the increased occurrence of failure in the CF/epoxy adherend (understood as a sign of thermal degradation) at higher displacement values (see Fig. 8). The drop in LSS did however only became significant once most of the failure occurred in the CF/epoxy adherend (0.38 mm displacement) as shown in Fig. 7. The existence of flow, and hence higher temperatures, close enough to the epoxy resin to alter the epoxy-PEI interphase (Fig. 4a) is likely linked to the CF/epoxy material becoming the major locus of failure. Note that specimens that failed solely in the CF/PEEK adherend, showed signs of sufficient adhesion, i.e., almost fully welded areas, and broken fibres and matrix failure upon testing. Thus, the change in the failure locus is believed to be related to some sort of degradation in the CF/epoxy adherend and not in differences in the interlaminar shear strength of the dissimilar adherends.

The reference PEEK-PEEK specimens showed a similar trend for the evolution of LSS with decreasing weld line thickness, i.e., increasing

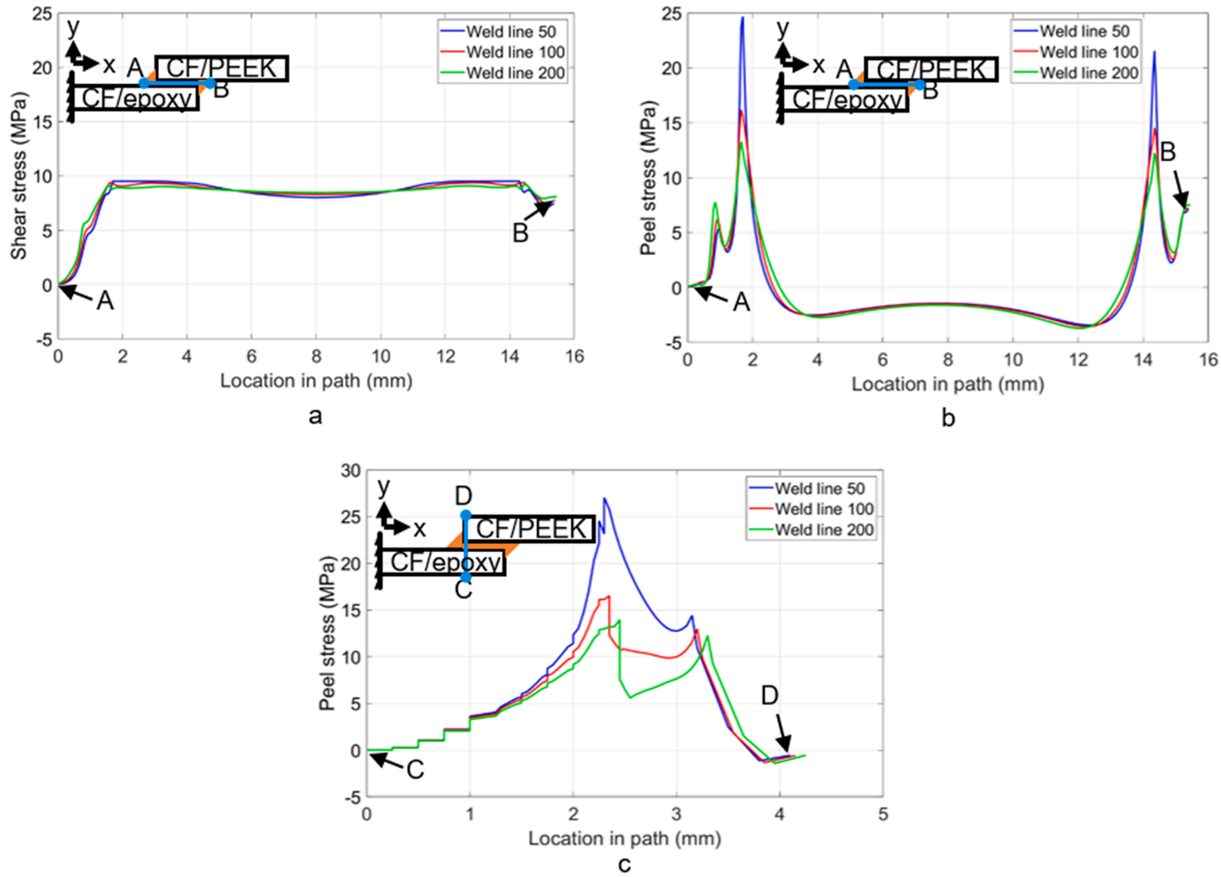

Fig. 6. Stresses obtained from the FE-model. a) Shear stresses along the AB path, b) peel stresses along the AB path and c) peel stresses along the CD path. (For interpretation of the references to color in this figure legend, the reader is referred to the web version of this article.)

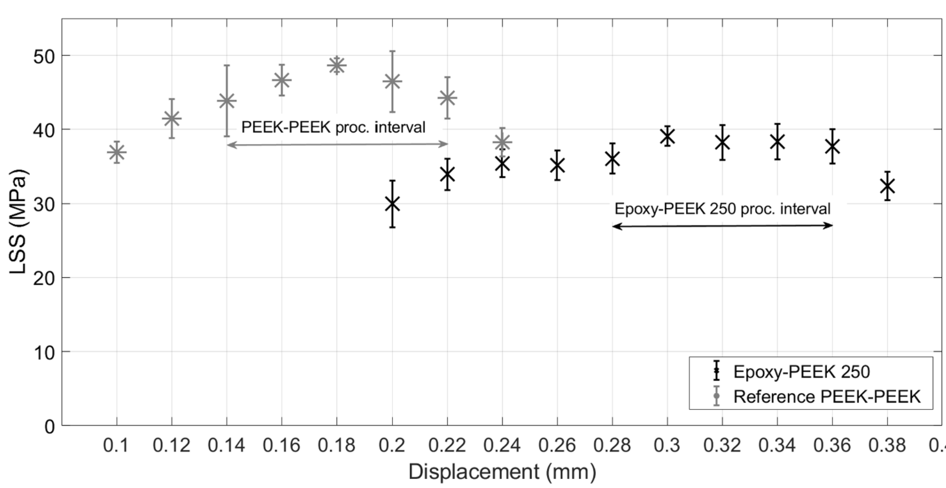

Fig. 7. Average lap shear strength of the epoxy-PEEK 250 and reference PEEK-PEEK configurations versus sonotrode displacement. The processing intervals were defined based on average LSS values higher than 90% of the maximum achieved LSS within the configuration.

displacement (see Fig. 5). The initial increase in LSS was also attributed to an increase in the amount of welded area (see Fig. 10). The subsequent decrease in LSS was however attributed to potentially higher stresses in the weld line together with the effects of significant resin squeeze-out in the adherends at higher displacement values. These effects were fibre distortion at the edges of the overlap and potential porosity in the layers adjacent to the overlap [16] which diverted failure from the first ply to deeper plies in the adherend (see Fig. 10). Contrarily, in the epoxy-PEEK 250 configuration the failure locus shifted to failure in the CF/epoxy adherend, before too much squeeze-out of the PEEK matrix could occur.

Another interesting difference between the epoxy-PEEK 250 and the reference PEEK-PEEK configurations was that the fracture surfaces corresponding to the epoxy-PEEK 250 configuration that resulted in maximum LSS were less textured than those of the reference PEEK-PEEK configuration which resulted in maximum LSS (e.g. see Fig. 9a and Fig. 11). Indeed, the cross-section micrographs in Fig. 3b for an epoxy-PEEK 250 joint welded at 0.30 mm displacement (i.e., displacement

Table 4
Results regarding the processing intervals of the epoxy-PEEK 250 and PEEK-PEEK configurations. The threshold LSS was defined as 90% of the LSS_{max}.

	Epoxy-PEEK 250	PEEK-PEEK
LSS_{max} (average ± stdv, MPa)	39.1 ± 1.3	48.7 ± 0.9
Threshold LSS (MPa)	35.2	43.8
d_{low} (mm) (heating time average ± stdv, ms)	0.28 (441 ± 28)	0.14 (444 ± 32)
d_{opt} (mm) (heating time, average ± stdv,ms)	0.30 (461 ± 38)	0.18 (609 ± 37)
d_{high} (mm), (heating time average ± stdv, ms)	0.36 (607 ± 46)	0.22 (685 ± 45)
Width of processing interval (mm)	0.08	0.08

which led to maximum LSS, see Table 4) shows that most of the weld line was composed of PEI. One could then think that the relatively flat fracture surfaces observed in that case resulted from failure at the interface between the PEI weld line and the CF/PEEK adherend. Likewise, occasional fibre breakage in the epoxy-PEEK 250 configuration (Fig. 9a) could have been the result of the flow of PEI within the first layer in the CF/PEEK adherend (see Fig. 3b). It should be noted that despite the fact that temperatures at the welding interface exceeded the melting temperature of PEEK [14] and that PEEK and PEI are known to be miscible in those conditions [20], a clear boundary could still be seen between both resins at the weld line (Figs. 3 and 15). Our hypothesis is that inter-diffusion between PEEK and PEI did happen but only locally at the boundary between the two. An overall polymer blend was hence not obtained since the welding process did not create the adequate mixing conditions for blending to occur. In the reference PEEK-PEEK configuration the weld line was of the same material as the matrix in the adherends, hence they lacked a well-defined, relatively flat path for failure to occur. The more tortuous failure path, consistent with more textured fracture surfaces, might have been one contributing factor to the higher average LSS of the PEEK-PEEK. Another possible factor that might have contributed to the different LSS values is the stiffness mismatch between the CF/PEEK and CF/epoxy adherends potentially inducing premature failure in the presumably less stiff CF fabric/PEEK material, as opposed to the PEEK-PEEK joints in which both adherends had a fabric reinforcement

5.2. Processing intervals

Despite the differences in the constituents and the mechanical performance of the epoxy-PEEK 250 and reference PEEK-PEEK configurations, their displacement-wise processing intervals were found to have the same width, i.e., 0.08 mm. However, there were some differences between these configurations. Firstly, the processing interval of the epoxy-PEEK 250 joints was shifted towards higher displacement values than that of the reference PEEK-PEEK joints. This behaviour is consistent with higher initial thickness of the neat resin layers between the composite material in the adherends prior to the welding process but rather similar final thicknesses of the weld line (see Fig. 3b and Fig. 4b). Note that a direct correlation between the initial thickness of the resin-rich layers, the displacement of the sonotrode during the vibration phase and the thickness of the weld line is not possible since the sonotrode continues to travel downwards during the consolidation phase. Secondly, when translating the limits of the processing interval into average heating times (see Table 4), the lower limit was similar in both configurations. The higher time limit was however around 13% lower for the epoxy-PEEK 250 joints, a difference which was statistically significant (($F(1,9) = 7.99$, $p = 0.02$). The shorter time-wise processing interval of the epoxy-PEEK 250 configuration is consistent with higher squeeze-out rates, i.e. faster vertical displacement of the sonotrode after the initial plateau, observed in the welding processes (see Fig. 14). These higher squeeze-out rates can be explained by a potentially faster temperature rise in the ED owing to: (i) additional heat generated by the coupling layer (together with the ED, which was the same in both epoxy-PEEK and PEEK-PEEK configurations) and (ii) thermal insulation between ED and carbon fibres in the CF/epoxy adherend provided by the coupling layer. This might also explain why at d_{opt} most of the ED was squeezed-out from the epoxy-PEEK 250 joints (see Fig. 3b) whereas that was not the case in the reference PEEK-PEEK joints (see Fig. 4b). Additionally, the shorter time-wise processing interval of the epoxy-PEEK 250 configuration is consistent with the higher sensitivity of the

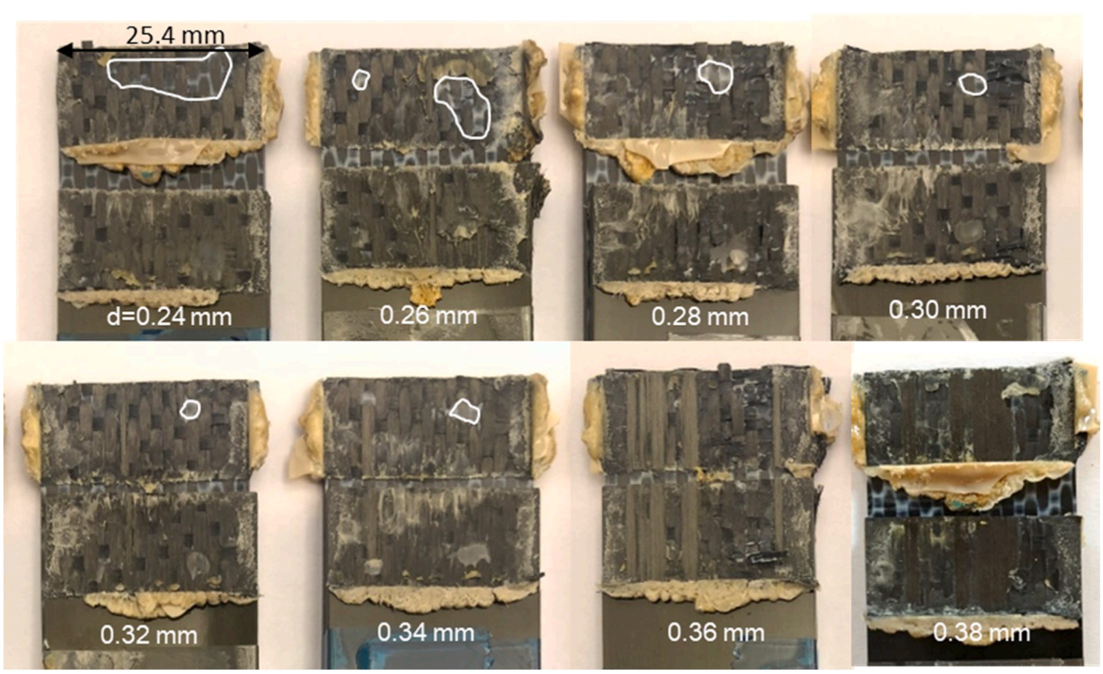

Fig. 8. Representative fracture surfaces of epoxy-PEEK 250 samples welded at different displacement values. The 0.28 mm, 0.30 mm and 0.36 mm values correspond to d_{low}, d_{opt} and d_{high}, respectively. The size of the unwelded areas (highlighted with white lines) decreased with an increasing target displacement. Welding at and above d_{high} resulted in failure in both adherends. (For interpretation of the references to color in this figure legend, the reader is referred to the web version of this article.)

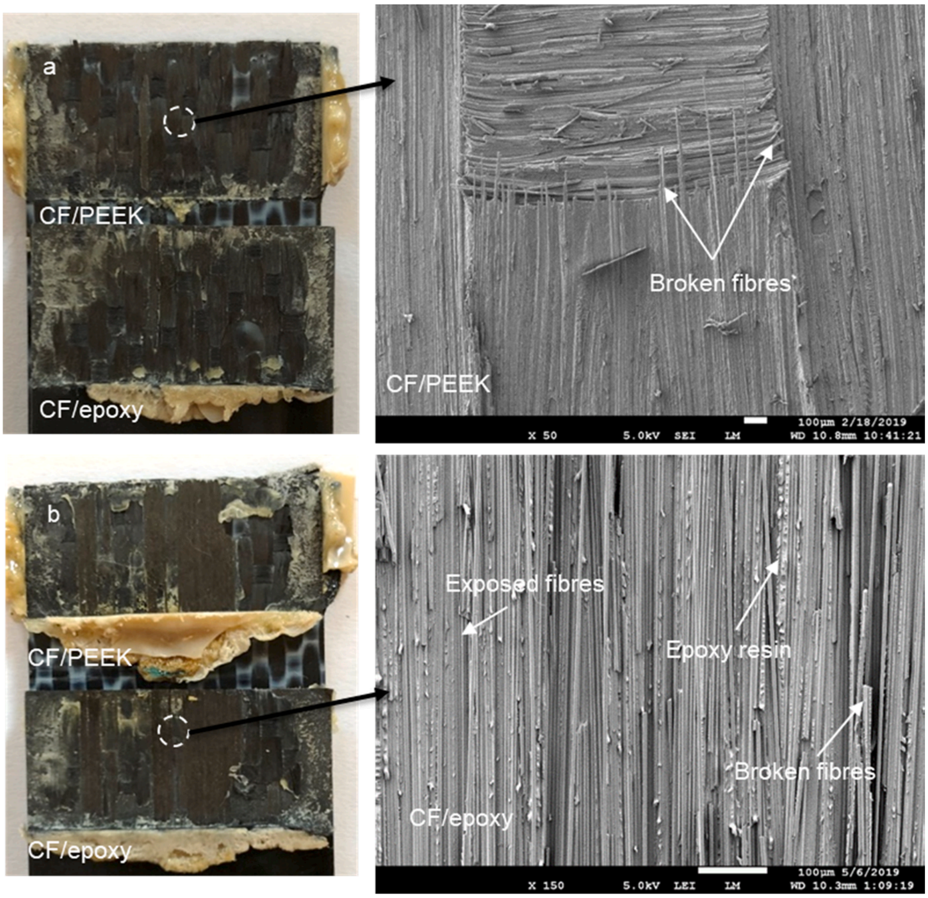

Fig. 9. Closer inspection of the fracture surfaces of epoxy-PEEK 250 joints welded at a) 0.30 mm, i.e., $d_{opt.}$ showing failure in the CF/PEEK adherend, characterized by resin-rich fibre bundles, ruptured PEEK matrix, and broken fibres and b) at 0.38 mm, i.e. right above d_{high}, depicting failure in both adherends with failure in the CF/epoxy adherend characterized by mainly exposed fibres and broken fibres. The SEM images are representative of the whole area in which either type of failure occurred. (For interpretation of the references to color in this figure legend, the reader is referred to the web version of this article.)

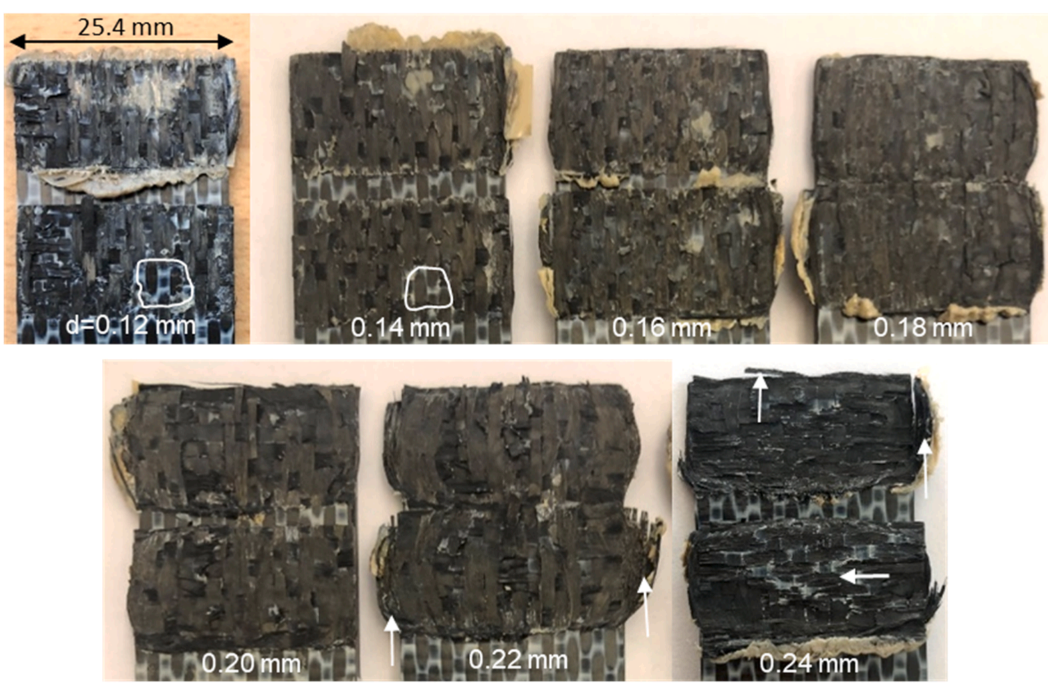

Fig. 10. Representative fracture surfaces of reference PEEK-PEEK samples welded at different displacement values. The displacement values of 0.14 mm, 0.18 mm and 0.22 mm correspond to the d_{low}, d_{opt}, and d_{high}, respectively. The size of the unwelded areas decreased with an increased target displacement. The unwelded areas are highlighted with white lines. The vertical arrows point at locations where significant fibre squeeze out was observed. The parallel arrow indicates failure between the first and second ply. (For interpretation of the references to color in this figure legend, the reader is referred to the web version of this article.)

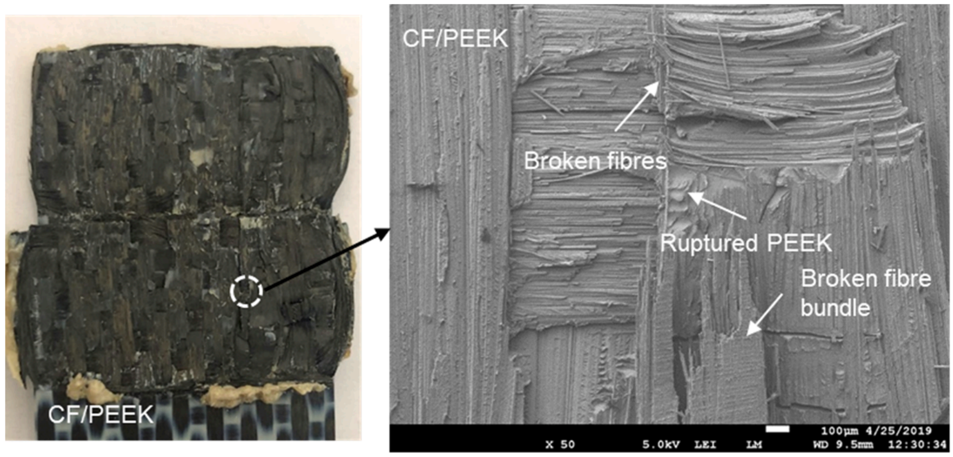

Fig. 11. Closer inspection of the fracture surfaces of a reference PEEK-PEEK sample welded at d_{opt}, showing failure in the CF/PEEK adherend, characterized by ruptured resin and broken fibres. The SEM image is representative of the whole overlap. (For interpretation of the references to color in this figure legend, the reader is referred to the web version of this article.)

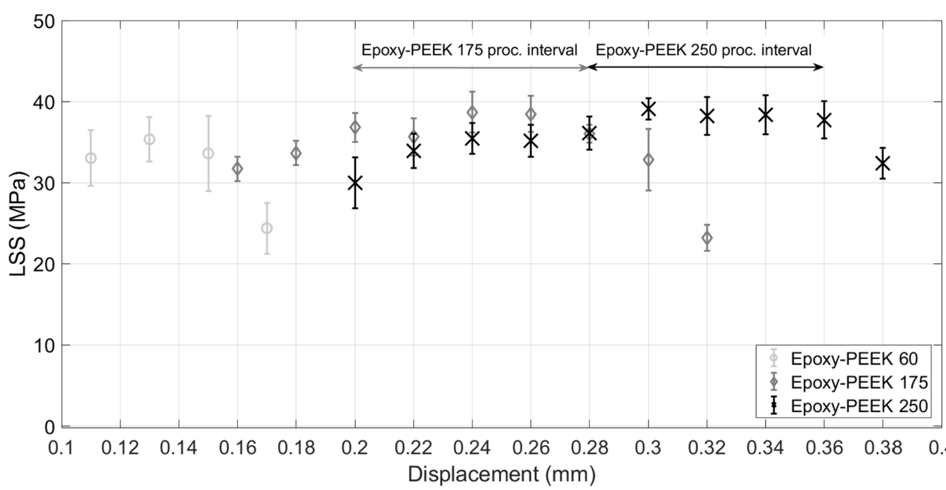

Fig. 12. Average lap shear strength of the epoxy-PEEK 250, epoxy-PEEK 175 and epoxy-PEEK 60 configurations versus the corresponding displacement.

Table 5
Results regarding the processing interval of the epoxy-PEEK 175 configuration.

LSS_{max} (average ± stdv, MPa)	38.7 ± 2.5
Threshold LSS (MPa)	35.2
d_{low} (mm) (heating time average ± stdv, ms)	0.20 (449 ± 22)
d_{opt} (mm) (heating time, average ± stdv,ms)	0.24 (462 ± 67)
d_{high} (mm), (heating time average ± stdv, ms)	0.28 (547 ± 34)
Width of processing interval (mm)	0.08

CF/epoxy material to the high temperatures developed during the welding process which eventually leads to thermal degradation and a shift in the failure mode (see Figs. 8 and 9).

Decreasing the thickness of the coupling layer from 250 to 175 μm neither affected the displacement-wise width of the processing interval nor the maximum average LSS (see Fig. 12). The processing interval of the epoxy-PEEK 175 configuration was however shifted towards lower displacement values. As in the comparison between the epoxy-PEEK 250 and the reference PEEK-PEEK configurations, this is consistent with lower initial thickness of the neat resin layers between the composite adherends prior to the welding process together with similar final thickness of the weld line (see Figs. 3 and 15). Finally, decreasing the thickness of the coupling layer did not have a significant effect on the time-wise width of the processing interval ($F(1,7) = 4.55, p = 0.07$). This is consistent with similar squeeze-out rates (see Fig. 14) and similar thicknesses of the coupling layer during the welding process, hence similar thermal barrier effect (see Figs. 3 and 15). This explanation is also supported by the preliminary temperature measurements in Fig. 16 which show similar temperature values at d_{high} for the epoxy-PEEK 250 and the epoxy-PEEK 175 configurations. Note that for these temperature measurements K-type thermocouples with 100 μm diameter were placed in between the CF/epoxy adherend and the coupling layer prior to the co-curing process. It should also be noted that only one temperature measurement experiment was performed per configuration to obtain these preliminary results. Further experiments are needed to confirm the trends observed in Fig. 16. Further decreasing the thickness of the coupling layer to 60 μm, decreased its efficiency as a thermal barrier significantly, as also indicated by the relatively higher temperatures reached in the epoxy-PEEK 60 configuration. As a result, it was not possible to obtain fully welded overlaps without causing thermal degradation in the CF/epoxy adherend.

5.3. Further discussion

Lastly, it is interesting to note that, despite the various differences among the epoxy-PEEK 250, epoxy-PEEK 175 and reference PEEK-PEEK configurations, the time to reach d_{low} was similar in all cases. This might suggest that exposure time of the CF/PEEK adherend to the molten PEEK ED plays a major role in achieving an almost fully welded overlap.

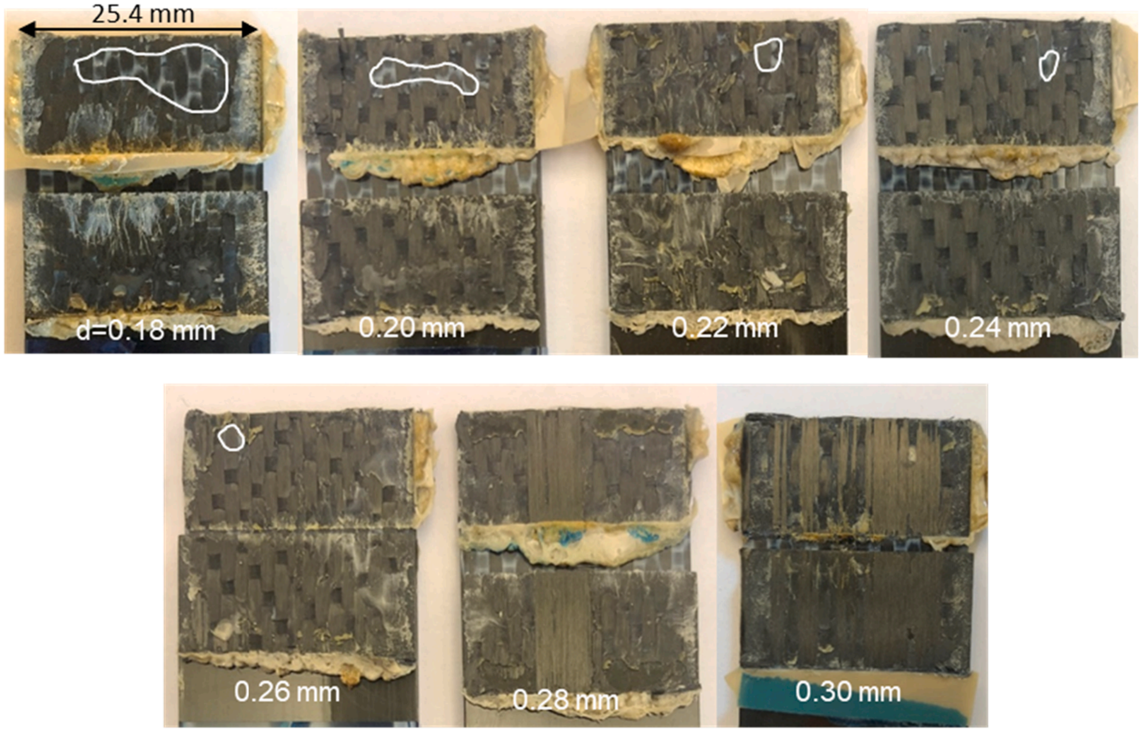

Fig. 13. Representative fracture surfaces of epoxy-PEEK 175 samples welded at different displacement values. The displacement values of 0.20 mm, 0.24 mm and 0.28 mm correspond to the d_{low}, d_{opt}, and d_{high}, respectively. (For interpretation of the references to color in this figure legend, the reader is referred to the web version of this article.)

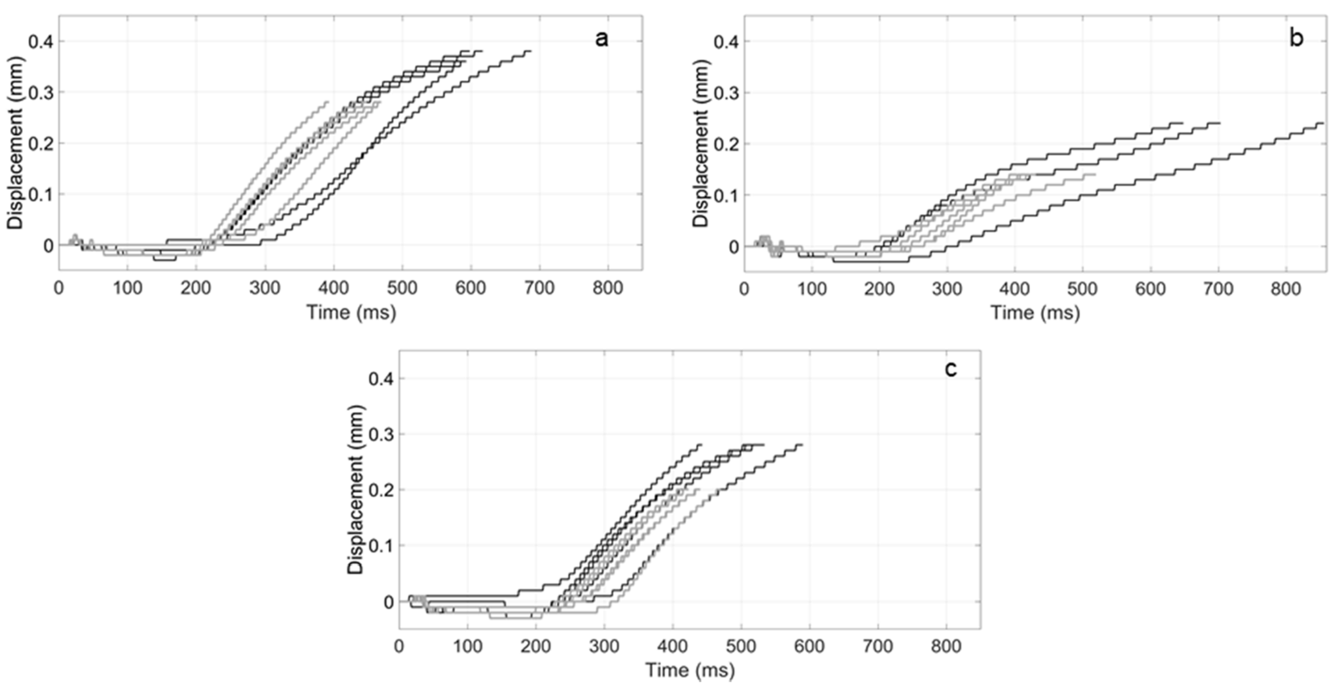

Fig. 14. Displacement of the sonotrode during the welding process in the a) epoxy-PEEK 250, b) reference PEEK-PEEK and c) epoxy-PEEK 175 configurations. Note: grey curves correspond to specimens welded up to d_{low}; black curves correspond to specimens welded up to d_{high} (see Table 4).

Furthermore, the fact that the displacement-wise width of the processing interval was similar in all three configurations suggests that the decrease in the thickness of the weld line might play a major role in defining the point at which the strength of the welded joint starts to degrade. However, these are only preliminary hypotheses that should be investigated in future research.

6. Conclusions

This paper presented a study on the effect of the heating time on the meso and microstructure of CF/epoxy to CF/PEEK joints ultrasonically welded through a PEI coupling layer and its relationship with the weld strength. Furthermore, processing intervals were defined with respect to

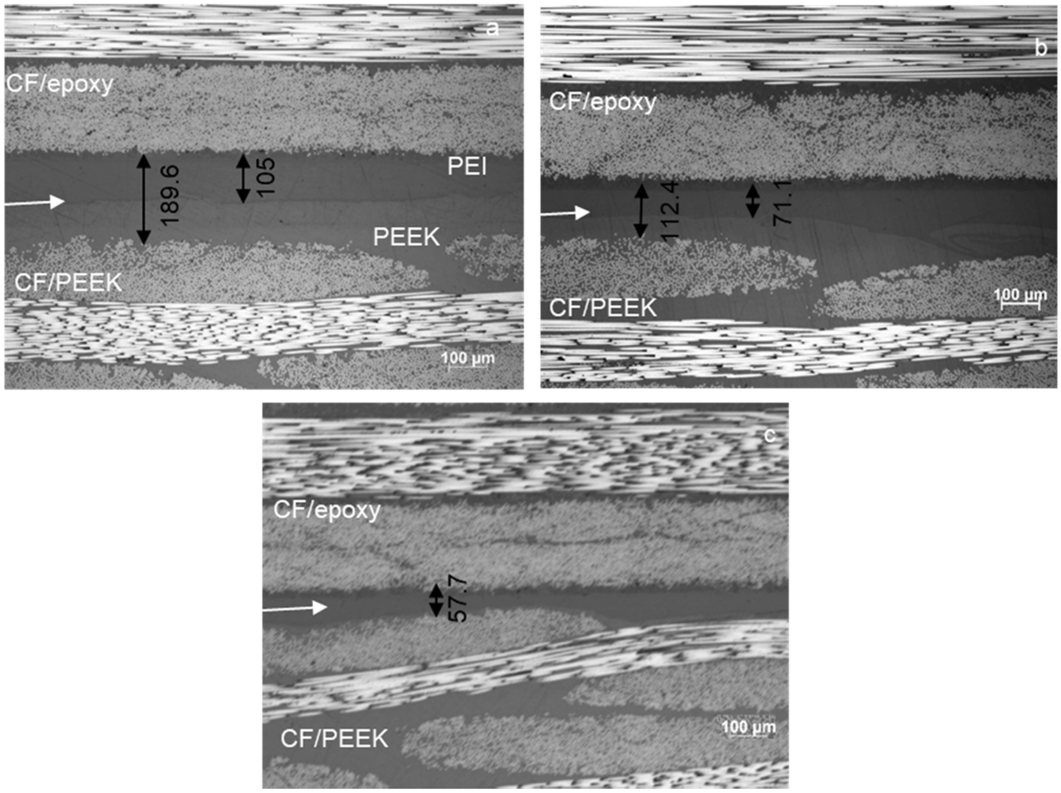

Fig. 15. Cross sections of epoxy-PEEK 175 samples welded at a displacement of a) 0.16 mm, b) 0.24 mm and c) 0.30 mm. White arrows indicate the weld line. The thickness measurements shown in the graphs are in μm.

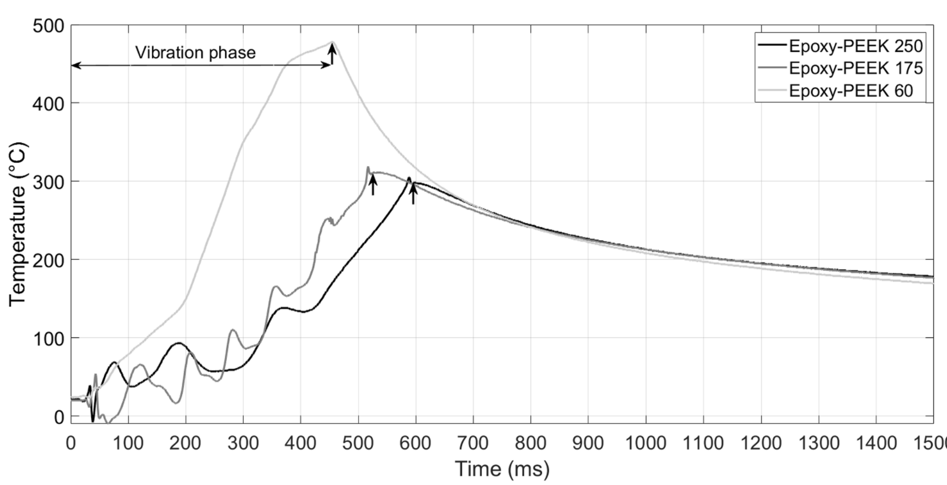

Fig. 16. Temperature evolution between the coupling layer and the CF/epoxy adherend for the considered epoxy-PEEK configurations. The samples were welded at d_{high}. Vertical arrows indicate the end of the vibration phase. Each sample contained one K-type thermocouple located at the middle of the overlap. The temperature was measured at 1000 Hz sampling rate.

the shortest and longest heating times that resulted in a minimum certain weld strength for different coupling layer thicknesses as well as for reference CF/PEEK to CF/PEEK welded joints. The main observations and conclusions drawn from this study are as follows:

- Increasing the heating time during welding of CF/epoxy and CF/PEEK adherends was found to decrease the weld line thickness (through combined flow of the PEEK energy director and the PEI coupling layer) and, ultimately, to promote flow in the epoxy-PEI gradient interphase. On the other hand, increasing the heating time caused the weld strength to increase up to a maximum and subsequently decrease. Even though the decrease in weld line thickness could be expected to have an effect on the stresses developed during the welding process, other factors were believed to significantly contribute to the variations in weld strength. In particular, the gradual increase in welded area (strength increase) and thermal effects in the CF/epoxy material (strength decrease). Similar conclusions were drawn from the study of reference CF/PEEK to CF/PEEK welded joints, although in that case the thermal effects linked to strength decrease were in the CF/PEEK material (fibre distortion and potential through the thickness porosity).

Fractographic analysis of the welded joints was an essential tool to establish those connections.

- Despite the sensitivity of the CF/epoxy adherend to high temperatures, a relatively wide processing interval was found for the epoxy-PEEK welds provided with a 250 μm-thick coupling layer. In terms of displacement of the sonotrode (used as the controlling parameter for the welding process), the processing interval of the epoxy-PEEK 250 joints was as wide as the processing interval of the reference PEEK-PEEK joints, both of them amounting to 0.08 mm. However, when translating the displacement values into average heating times, the reference PEEK-PEEK joints were able to withstand longer heating times than the epoxy-PEEK 250 ones, consistent with the higher sensitivity of the former to thermal degradation.
- Decreasing the thickness of the coupling layer from 250 μm to 175 μm did not affect the sensitivity of the welding process to the displacement or heating time. However, further decreasing the thickness of the coupling layer to 60 μm resulted in a decrease of the achievable LSS and the appearance of thermal degradation signs even before fully welded overlaps could be obtained.

CRediT authorship contribution statement

Eirini Tsiangou: Conceptualization, Methodology, Validation, Investigation, Writing - original draft, Visualization, Writing - review & editing. **Julian Kupski:** Methodology, Software, Validation, Visualization, Writing - review & editing. **Sofia Teixeira Freitas:** Writing - review & editing, Funding acquisition, Supervision. **Rinze Benedictus:** Writing - review & editing, Supervision. **Irene Fernandez Villegas:** Conceptualization, Writing - review & editing, Funding acquisition, Supervision.

Declaration of Competing Interest

The authors declare that they have no known competing financial interests or personal relationships that could have appeared to influence the work reported in this paper.

Acknowledgements

This research is part of the European project EFFICOMP that focuses on efficient manufacturing of composite parts. The EFFICOMP project received funding from the European Union Horizon 2020 research and innovation program under grant agreement No. 690802.

References

[1] Ageorges C, Ye L, Hou M. Advances in fusion boding techniques for joining thermoplastics materials composites: a review. Compos Part A Appl Sci Manuf 2001;32:839–57.
[2] Villegas IF, van Moorleghem R. Ultrasonic welding of carbon/epoxy and carbon/PEEK composites through a PEI thermoplastic coupling layer. Compos Part A Appl Sci Manuf 2018;109:75–83.
[3] Hou M. Thermoplastic adhesive for thermosetting composites. Mater Sci Forum 2012;706–709:2968–73.
[4] Hou M. Fusion bonding of carbon fiber reinforced epoxy laminates. Adv Mater Res 2013:626.
[5] Paton R, Hou M, Beehag A, Falzon P. A breakthrough in the assembly of aircraft composite structures. 25th Congr. Int. Counc. Aeronaut. Sci.. 2006.
[6] Don RC, McKnight H, Wetzel ED, Gillespie Jr JW. Application of thermoplastic resistance welding techniques to thermoset composites. Annu Tech Conf Soc Plast 1994:1295–7.
[7] Ageorges C, Ye L. Resistance welding of thermosetting composite/thermoplastic composite joints. Adv Mater 2006;32.
[8] McKnight SH, Holmes ST, Gillespie JW, Lambing CLT, Marinelli JM. Scaling Issues in Resistance- Welded Thermoplastic Composite Joints. Adv Polym Technol 1997; 16:279–95.
[9] Schieler O, Beier U. Induction welding of hybrid thermoplastic-thermoset composite parts. Int J Appl Sci Technol 2016;9:27–36.
[10] Lionetto F, Morillas MN, Pappadà S, Buccoliero G, Villegas IF, Maffezzoli A. A Hybrid welding of carbon-fiber reinforced epoxy based composites. Compos Part A 2018;104:32–40.
[11] Beiss T, Menacher M, Feulner R, Huelder G, Osswald TA. Vibration joining of fiber-reinforced thermosets. Polym Compos 2010;31:1205–12.
[12] Villegas IF, Rubio PV. On avoiding thermal degradation during welding of high-performance thermoplastic composites to thermoset composites. Compos Part A Appl Sci Manuf 2015;77:172–80.
[13] Tsiangou E, Teixeira de Freitas S, Villegas IF, Benedictus R. Investigation on energy director-less ultrasonic welding of polyetherimide (PEI)- to epoxy-based composites. Compos Part B Eng 2019;173.
[14] Tsiangou E, Teixeira de Freitas S, Villegas IF, Benedictus R. Ultrasonic welding of epoxy- to polyetheretherketone- based composites: Investigation on the material of the energy director and the thickness of the coupling layer. J Compos Mater 2020; 54.
[15] Villegas IF. Ultrasonic welding of thermoplastic composites. Front Mater 2019;6: 1–10. https://doi.org/10.3389/fmats.2019.00291.
[16] Villegas IF. Strength development versus process data in ultrasonic welding of thermoplastic composites with flat energy directors and its application to the definition of optimum processing parameters. Compos Part A Appl Sci Manuf 2014; 65:27–37.
[17] Hou M, Ye L, Mai Y-W, Yuan Q. Manufacturing and joining of advanced thermoplastic composites. In: ICCM-13, Beijing, China; 2001.
[18] Gleich DM, Van Tooren MJL, Beukers A. Analysis and evaluation of bondline thickness effects on failure load in adhesively bonded structures. J Adhes Sci Technol 2001;15:1091–101.
[19] Camanho PP, Dávila CG, Pinho ST, Iannucci L, Robinson P. Prediction of in situ strengths and matrix cracking in composites under transverse tension and in-plane shear. Compos Part A Appl Sci Manuf 2006;37(2):165–76.
[20] Torre L, Kenny JM. Blends of semicrystalline and amorphous polymeric matrices for high performance composites. Polym Compos 1992;13:380–5. https://doi.org/10.1002/pc.750130507.